Supporting Information for:

Single Molecule Rectification Induced by the Asymmetry of a Single Frontier Orbital

Wendu Ding, Christian F. A. Negre,* Leslie Vogt, and Victor S. Batista*

Department of Chemistry, Yale University, P.O. Box 208107, New Haven, CT 06520-8107, and Energy Sciences Institute, Yale University, P.O. Box 27394, West Haven, CT 06516-7394

E-mail: christian.negre@yale.edu; victor.batista@yale.edu

1 Transmission Function: Tight-Binding Model

This section provides a derivation of Eq. (1) of the main text, giving an expression for the transmission function as a function of the applied bias potential for a tight binding model with a single transport channel. The Green's function for such a molecule in between the electron source and drain reservoirs (Figure S1) is

$$\mathscr{G}_{dev}(\varepsilon) = [\varepsilon - H_{dev} - \Sigma_T(\varepsilon)]^{-1} \tag{1}$$

where ε is the energy, H_{dev} is the molecular Hamiltonian, and Σ_T is the total self-energy of the contacts, which can be decomposed as the sum of the self-energy of the left and right lead contributions: $\Sigma_T(\varepsilon) = \Sigma_L(\varepsilon) + \Sigma_R(\varepsilon)$.

*To whom correspondence should be addressed

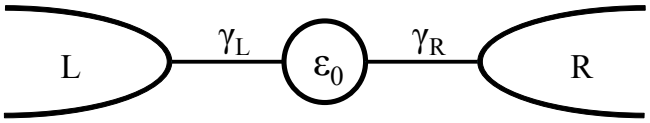

Figure S1: Scheme of a molecule with a single transport channel state $|\varepsilon_0\rangle$, coupled to the left (L) and right (R) electron reservoirs with coupling constants γ_L and γ_R, respectively.

The retarded and advanced Green's functions are

$$\mathscr{G}^{+}_{dev}(\varepsilon) = \frac{1}{\varepsilon - H_{dev} - \Sigma_T(\varepsilon)} \tag{2}$$

$$\mathscr{G}^{-}_{dev}(\varepsilon) = \frac{1}{\varepsilon - H_{dev} - \Sigma^{\dagger}_T(\varepsilon)} \tag{3}$$

The self-energy for the left (L) and right (R) contacts are

$$\Sigma_{L/R}(\varepsilon) = \Delta_{L/R} + i\Gamma_{L/R}(\varepsilon) \tag{4}$$

where the real part Δ can be approximated as $\Delta_L \simeq \frac{V}{2}$ and $\Delta_R \simeq -\frac{V}{2}$, with V the applied bias voltage. The total self-energy is

$$\Sigma_T(\varepsilon) \simeq i[\Gamma_L(\varepsilon) + \Gamma_R(\varepsilon)] \tag{5}$$

Considering there is only one state $|\varepsilon_0\rangle$ between the two contacts, we have $\langle\varepsilon_0|H_{dev}|\varepsilon_0\rangle = \varepsilon_0$, and the retarded and advanced Green's function take the form:

$$\mathscr{G}^{+}_{dev}(\varepsilon) = \frac{1}{\varepsilon - \varepsilon_0 - i[\Gamma_L(\varepsilon) + \Gamma_R(\varepsilon)]} \tag{6}$$

$$\mathscr{G}^{-}_{dev}(\varepsilon) = \frac{1}{\varepsilon - \varepsilon_0 + i[\Gamma_L(\varepsilon) + \Gamma_R(\varepsilon)]} \tag{7}$$

For either the left or right contact:

$$\Sigma(\varepsilon)_{L/R} = \gamma^{\dagger}_{L/R}\mathscr{G}^{+}_{L/R}\gamma_{L/R} = \gamma^{2}_{L/R}\mathscr{G}^{+}_{L/R} \tag{8}$$

where $\gamma_{L/R}$ is the coupling between the contact and the device, and $\mathscr{G}^{+}_{L/R}$ is the retarded Green's

function of the contact. The seccond equality results from the fact that $\gamma_{L/R}$ and $\mathscr{G}^{+}_{L/R}$ commute in this particular case. Together with the expression $\Sigma(\varepsilon)_{L/R} = \Delta_{L/R} + i\Gamma_{L/R}(\varepsilon)$, we have:

$$\begin{aligned} &\Delta_{L/R} + i\Gamma(\varepsilon)_{L/R} = \gamma^2_{L/R}\mathscr{G}^{+}_{L/R}(\varepsilon) \\ &\implies \mathscr{G}^{+}_{L/R}(\varepsilon) = \frac{\Delta_{L/R}}{\gamma^2_{L/R}} + i\frac{\Gamma_{L/R}(\varepsilon)}{\gamma^2_{L/R}} \end{aligned} \tag{9}$$

The density of states (DOS) of the contact can be expressed by the imaginary part of the retarded Green's function of the contact: [1,2]

$$DOS(\varepsilon) = -\frac{1}{\pi} Im[\mathscr{G}^{+}(\varepsilon)] \tag{10}$$

therefore, we can write the imaginary part of the self-energy $\Gamma_{L/R}$ in terms of the contact DOS:

$$\begin{aligned} DOS_{L/R}(\varepsilon) = -\frac{1}{\pi} Im[\mathscr{G}^{+}_{L/R}(\varepsilon)] = -\frac{1}{\pi}\frac{\Gamma(\varepsilon)_{L/R}}{\gamma^2_{L/R}} \\ \implies \Gamma(\varepsilon)_{L/R} = -\pi\gamma^2_{L/R} DOS_{L/R}(\varepsilon) \end{aligned} \tag{11}$$

Also,

$$\mathscr{A}_{L/R}(\varepsilon) = i[\Sigma_{L/R}(\varepsilon) - \Sigma^{\dagger}_{L/R}(\varepsilon)] = -2\Gamma_{L/R}(\varepsilon) \tag{12}$$

Therefore, the transmission function can be computed as:

$$\begin{aligned} T(\varepsilon) &= \mathscr{A}_L(\varepsilon)\mathscr{G}^{+}_{dev}(\varepsilon)\mathscr{A}_R(\varepsilon)\mathscr{G}^{-}_{dev}(\varepsilon) \\ &= 2\Gamma_L(\varepsilon)\mathscr{G}^{+}_{dev}(\varepsilon)2\Gamma_R(\varepsilon)\mathscr{G}^{-}_{dev}(\varepsilon) \\ &= \frac{4\Gamma_L(\varepsilon)\Gamma_R(\varepsilon)}{(\varepsilon-\varepsilon_0)^2 + [\Gamma_L(\varepsilon)+\Gamma_R(\varepsilon)]^2} \\ &= \frac{4\pi^2\gamma^2_L DOS_L(\varepsilon)\gamma^2_R DOS_R(\varepsilon)}{(\varepsilon-\varepsilon_0)^2 + \pi^2[\gamma^2_L DOS_L(\varepsilon) + \gamma^2_R DOS_R(\varepsilon)]^2} \end{aligned} \tag{13}$$

Under a voltage bias V, we have:

$$T(\varepsilon) = \frac{4\pi^2\gamma_L^2 DOS_L(\varepsilon - \frac{V}{2})\gamma_R^2 DOS_R(\varepsilon + \frac{V}{2})}{(\varepsilon - \varepsilon_0)^2 + \pi^2[\gamma_L^2 DOS_L(\varepsilon - \frac{V}{2}) + \gamma_R^2 DOS_R(\varepsilon + \frac{V}{2})]^2} \tag{14}$$

2 Non-rectifiers and comparison of dipole moments and polarizability

Here we show three examples (B1, B2, and B3) of intentionally designed asymmetrical molecules with large dipole moments and polarizability in the transport direction. Their I-V curves are shown in Figure S2, Figure S3, and Figure S4, respectively. By comparing rectification ratio, dipole moment, and polarizability among these molecules and the molecules in main text (see Table S1), there is no obvious correlation between rectification ratio and dipole moment or polarizability.

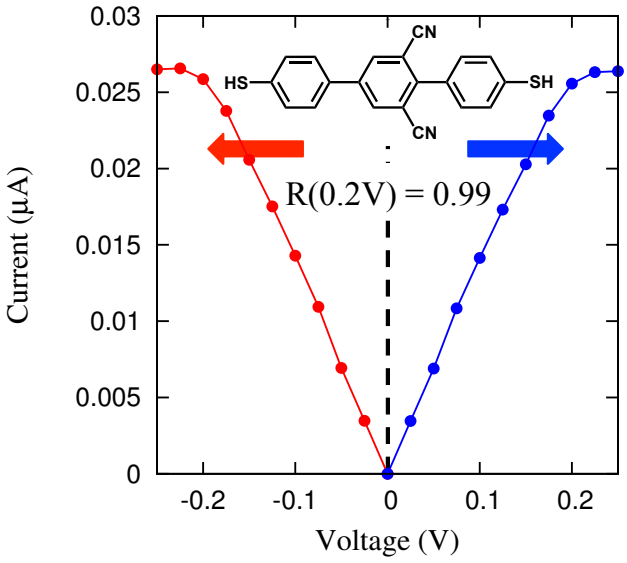

Figure S2: I-V curve for B1 (see inset for structure) and rectification ratio is 0.99.

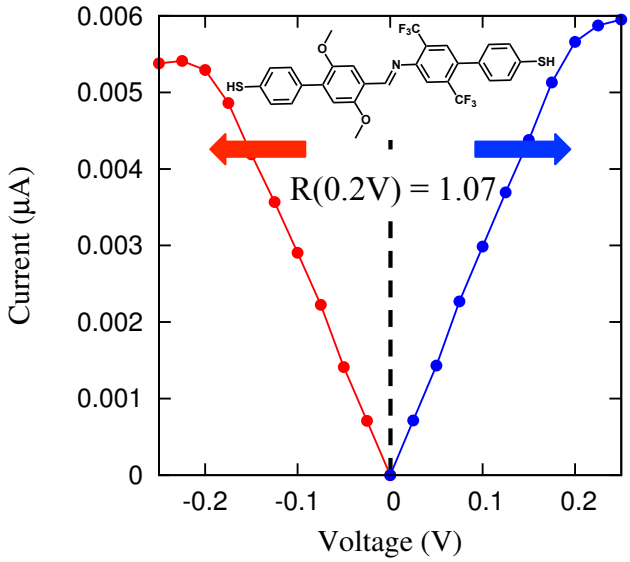

Figure S3: I-V curve for B2 (see inset for structure) and rectification ratio is 1.07.

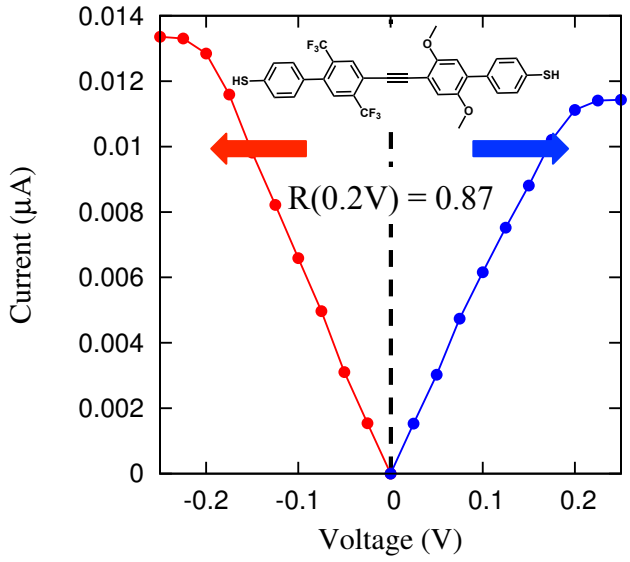

Figure S4: I-V curve for B3 (see inset for structure) and rectification ratio is 0.87.

Table S1: Comparison among molecules of their rectification ratio, dipole moment, and polarizability in the transport direction.

Molecule	Rectification Ratio	Dipole Moment (Debye)	Polarizability ($Bohr^3$)
A1	1.65	1.9427	381.038
A2	1.04	-0.1334	482.026
A3	1.51	-0.4068	381.087
B1	0.99	-3.5798	535.42
B2	1.07	-2.9421	915.32
B3	0.87	1.1900	991.945

3 Additional figures

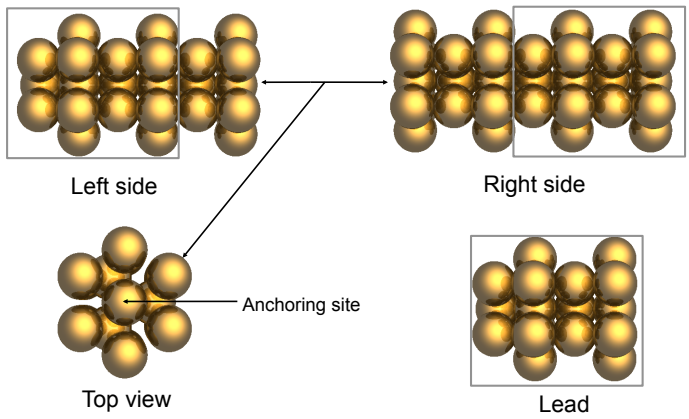

Figure S5: Nanowire hcp leads used for building the extended systems described in the text. These nanowire electrodes were modeled according to Krstić *et al.*[3–5] Each gold unit cell has two sublayers of seven and three gold atoms respectively, with periodic boundary conditions along the transport direction where the seven atom face mimics the gold (111) surface. The lattice constant is 4.080 Å.

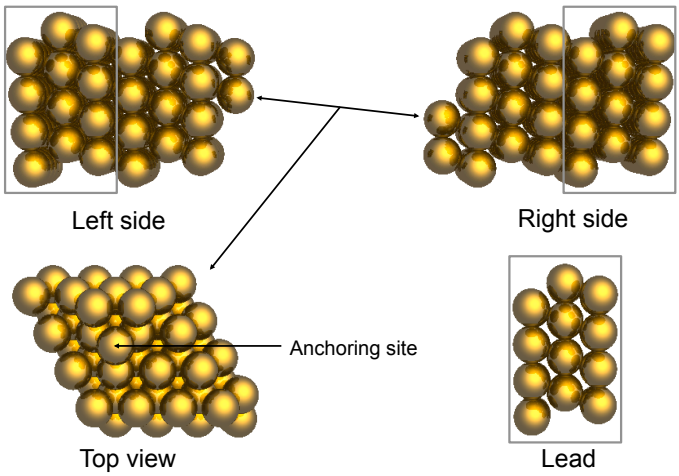

Figure S6: Slab fcc leads used for building the extended systems described in the text. These slab electrodes were modeled using 6 layers of 16 gold atoms cut from a fcc lattice, with periodic boundary conditions in all three dimensions. A single layer of a triad contact motif is added to attach the molecule.[6,7] The face of the leads is the (111) surface. The lattice constant of the fcc lattice is 4.080 Å.

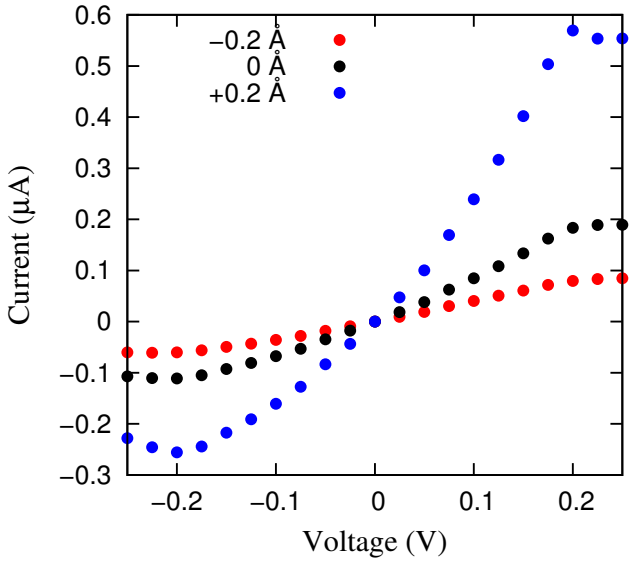

Figure S7: I-V curves for **Au$_L$-S-Ph-amide-Ph-S-Au$_R$** for various different S-Au distances.

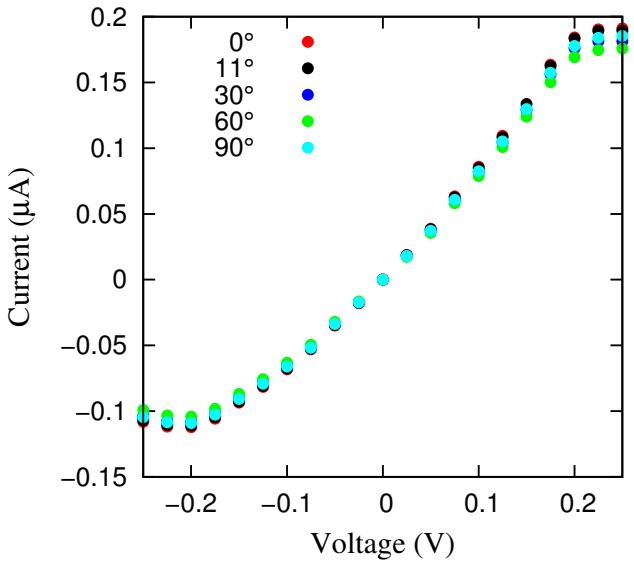

Figure S8: I-V curves for **Au**$_L$**-S-Ph-amide-Ph-S-Au**$_R$ for various rotational orientations of the molecule with respect to the contact.

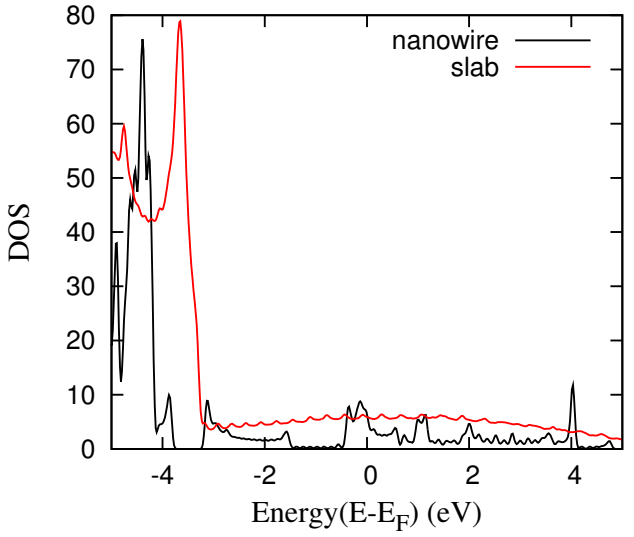

Figure S9: Density of states for nanowire and slab electrodes.

Table S2: Figures from the main text with y-axis values.

Figure 4a

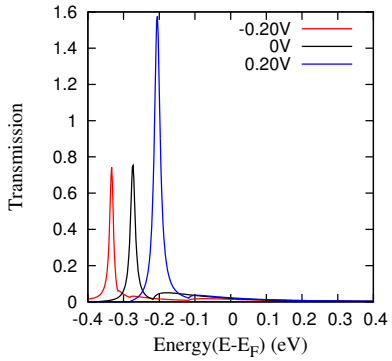

Figure4b

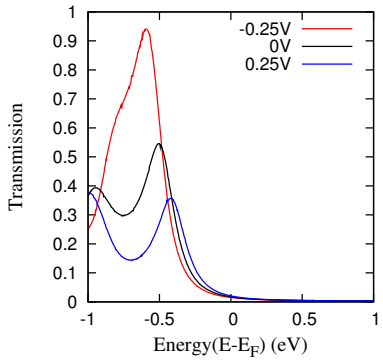

Figure 5a

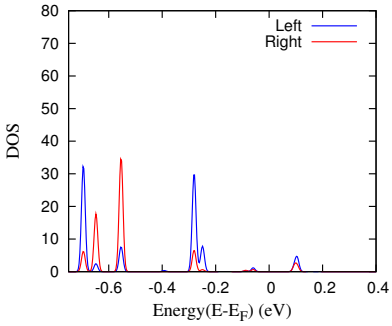

Figure 6

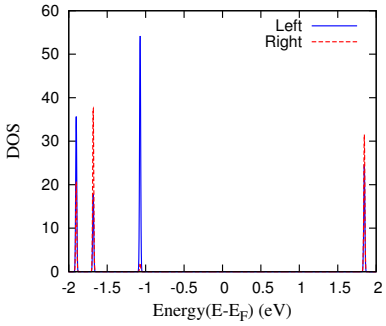

Figure 7a

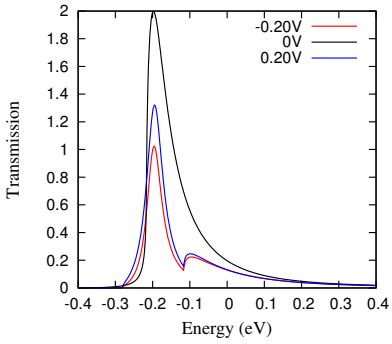

Figure 9a

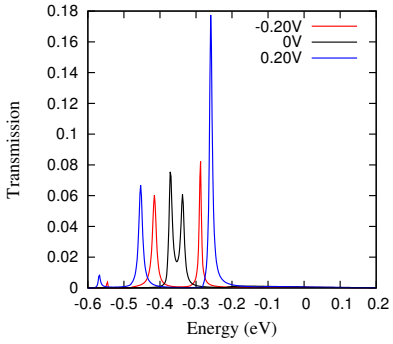

Figure 8

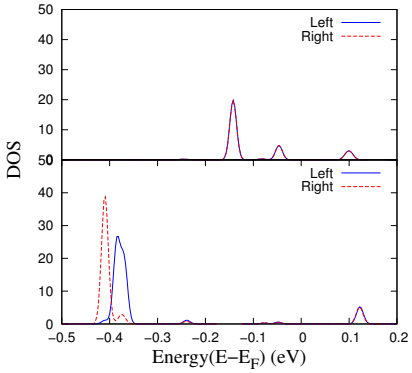

4 Coordinates of isolated studied systems

HS-Ph-amide-Ph-SH

C	-4.67450400	-0.20420200	-0.02467400
C	-3.94683100	-1.37807200	-0.25661100
C	-3.97529100	0.98643100	0.19883800
C	-2.55787700	-1.35169100	-0.26369100
H	-4.46321200	-2.31750500	-0.42910000
C	-2.58231400	1.01979600	0.19793000
H	-4.51604700	1.91156900	0.37587200
C	-1.85676200	-0.15745000	-0.03641000
H	-2.01053000	-2.27430200	-0.44378100
H	-2.05262700	1.94605300	0.36696900
N	-0.44817600	-0.21925000	-0.04407200
H	-0.06535500	-1.12745300	-0.26018600
C	0.46070200	0.80995600	0.07599500
O	0.14115700	1.99055500	0.17789900
C	1.90237500	0.39152300	0.05640800
C	2.84562000	1.36365600	-0.30164600
C	2.36007000	-0.88709700	0.40603100
C	4.20176300	1.06435900	-0.34469600
H	2.49064000	2.35922700	-0.54465400
C	3.71692900	-1.19356900	0.37559500
H	1.66776300	-1.65122300	0.74868600
C	4.65036000	-0.22121900	-0.00911500
H	4.91104300	1.83270500	-0.63736800
H	4.05145800	-2.18570700	0.66308500
S	-6.46079400	-0.30232900	-0.04553100
S	6.37123600	-0.68625000	-0.03993900
H	-6.69517500	0.96005400	0.36047800
H	6.85750900	0.51962300	-0.39088700

HS-stilbene-SH optimized structure

C	0.47890500	-0.47538500	0.00345300
C	1.92731500	-0.26994300	0.00606600
C	2.77580700	-1.38920900	-0.06945900
C	2.54100100	0.99647700	0.08251800
C	3.92175800	1.13386600	0.07667900
C	-1.92731100	0.27005100	0.00583500
C	-2.77637100	1.38995500	-0.07054300
C	-4.16061200	1.26307600	-0.07673900
C	-4.75058900	-0.00475600	-0.00324500
C	-3.92248000	-1.13392000	0.07803800

C	-2.54059100	-0.99547400	0.08304500
H	-4.78271700	2.15114300	-0.13898500
H	-4.35793200	-2.12702500	0.14100800
H	-1.93177000	-1.89117300	0.15416800
C	-0.47878900	0.47533900	0.00353700
C	4.16138900	-1.26321800	-0.07487800
C	4.75064400	0.00377100	-0.00307100
H	4.36185600	2.12504400	0.13643200
H	1.93187400	1.89195400	0.15218400
H	4.77942600	-2.15431300	-0.13464900
H	2.33757900	-2.38228500	-0.12724900
H	-2.33775500	2.38270200	-0.12923900
H	0.17707900	-1.52141000	-0.00721500
H	-0.17694600	1.52127300	-0.00666500
S	6.51738200	0.26104500	-0.00153000
S	-6.53308800	-0.10589100	-0.01224900
H	6.86950300	-1.03368900	-0.11836900
H	-6.61935100	-1.44845000	0.05164000

HS-stilbene-SH twisted structure

C	0.44773000	0.33651000	-0.00648200
C	1.91044200	0.19836200	-0.00507700
C	2.70345000	1.35748700	0.00064900
C	2.57832200	-1.04054200	-0.00893700
C	3.96454500	-1.11484200	-0.00613300
C	-1.93780700	-0.40060500	0.00034300
C	-2.65301300	-0.29528400	1.20227100
C	-4.02905500	-0.08047700	1.20830900
C	-4.73012600	0.03191800	0.00103000
C	-4.02987600	-0.07354600	-1.20597200
C	-2.65251700	-0.28907400	-1.20010200
H	-4.55685400	0.00160500	2.15407200
H	-4.55313100	0.01401200	-2.15382700
H	-2.12227700	-0.36754500	-2.14477900
C	-0.46848800	-0.64451900	0.00014900
C	4.09425000	1.29575100	0.00347600
C	4.74007300	0.05497200	0.00029400
H	4.44981100	-2.08651600	-0.00916900
H	2.00873300	-1.96450100	-0.01478300
H	4.67113000	2.21593900	0.00816300
H	2.21919300	2.33061900	0.00349000
H	-2.12243000	-0.37872100	2.14624000
H	0.08668100	1.36466900	-0.01269200
H	-0.15107700	-1.68762900	0.00989400

```
S                   6.51723700   -0.12038300    0.00329100
S                  -6.49533300    0.30916900    0.08077600
H                   6.80832300    1.19456300    0.01311700
H                  -6.71613600    0.32626800   -1.24770400
```

5 Sample imput file with the coordinates for the full system of Au_L-S-Ph-amide-Ph-S-Au_R

```
#  Sample input for the L-S-Ph-amide-Ph-S-R system

%block LatticeVectors
    30.000    0.000    0.00000
    0.000    30.000    0.00000
   0.00000    0.00000  45.74497
%endblock LatticeVectors


PAO.BasisType split
PAO.SplitNorm 0.15
%block    PAO.BasisSizes
    Au  DZ
    S   DZ
    C   DZ
    H   DZ
    N   DZ
    O   DZ
%endblock  PAO.BasisSizes
PAO.EnergyShift 0.01 eV

%block kgrid_Monkhorst_Pack
    1   0   0    0.0
    0   1   0    0.0
    0   0   1    0.0
%endblock kgrid_Monkhorst_Pack
BandLinesScale          ReciprocalLatticeVectors

XC.functional         GGA
XC.authors            PBE
MeshCutoff  200.0 Ry

ElectronicTemperature           300 K
```

```
MaxSCFIterations                30000
DM.MixingWeight                 0.02
DM.NumberPulay                  4
DM.Tolerance                    1.0D-5
DM.UseSaveDM                    T

SolutionMethod                  transiesta

TS.HSFileLeft   AuLeads.TSHS
TS.NumUsedAtomsLeft    20
TS.HSFileRight  AuLeads.TSHS
TS.NumUsedAtomsRight   20


TS.TBT.NPoints        1000
TS.TBT.Emin           -1.0 eV
TS.TBT.Emax             1.0 eV
TS.TBT.OutputRegionData False
TS.BiasContour.NumPoints 100
TS.ComplexContour.Emin  -20.0 Ry
TS.ComplexContour.NumCircle 100
TS.ComplexContour.NumLine  20
TS.ComplexContour.NumPoles 10
TS.BiasContour.Eta 10D-4  Ry
TS.Voltage VOLTAGE  eV


%block ChemicalSpeciesLabel
         1          79 Au
         2          16 S
         3           6 C
         4           1 H
         5           7 N
         6           8 O
%endblock ChemicalSpeciesLabel

AtomicCoordinatesFormat  Ang
%block AtomicCoordinatesAndAtomicSpecies
  -0.83280000   -1.44250000    0.00000000   1  Au   1
   1.66560000    0.00000000    0.00000000   1  Au   2
  -0.83280000    1.44250000    0.00000000   1  Au   3
   0.00000000   -2.88500000    2.35560000   1  Au   4
  -2.49850000   -1.44250000    2.35560000   1  Au   5
   2.49850000   -1.44250000    2.35560000   1  Au   6
   0.00000000    0.00000000    2.35560000   1  Au   7
  -2.49850000    1.44250000    2.35560000   1  Au   8
```

```
 2.49850000    1.44250000    2.35560000   1  Au   9
 0.00000000    2.88500000    2.35560000   1  Au  10
-0.83280000   -1.44250000    4.71120000   1  Au  11
 1.66560000    0.00000000    4.71120000   1  Au  12
-0.83280000    1.44250000    4.71120000   1  Au  13
 0.00000000   -2.88500000    7.06680000   1  Au  14
-2.49850000   -1.44250000    7.06680000   1  Au  15
 2.49850000   -1.44250000    7.06680000   1  Au  16
 0.00000000    0.00000000    7.06680000   1  Au  17
-2.49850000    1.44250000    7.06680000   1  Au  18
 2.49850000    1.44250000    7.06680000   1  Au  19
 0.00000000    2.88500000    7.06680000   1  Au  20
-0.83280000   -1.44250000    9.42240000   1  Au  21
 1.66560000    0.00000000    9.42240000   1  Au  22
-0.83280000    1.44250000    9.42240000   1  Au  23
 0.00000000   -2.88500000   11.77800000   1  Au  24
-2.49850000   -1.44250000   11.77800000   1  Au  25
 2.49850000   -1.44250000   11.77800000   1  Au  26
 0.00000000    0.00000000   11.77800000   1  Au  27
-2.49850000    1.44250000   11.77800000   1  Au  28
 2.49850000    1.44250000   11.77800000   1  Au  29
 0.00000000    2.88500000   11.77800000   1  Au  30
 0.00000000    0.00000000   14.09800000   2  S   31
-0.02008000   -0.15150000   15.88056000   3  C   32
-0.42057000   -2.27107000   15.97585000   4  H   33
 0.38445000    1.95454000   16.15478000   4  H   34
-0.24329000   -1.36252000   16.54395000   3  C   35
 0.21218000    1.00008000   16.64291000   3  C   36
-0.24178000   -1.43752000   17.93531000   3  C   37
 0.21987000    0.93217000   18.03045000   3  C   38
-0.41059000   -2.37921000   18.43713000   4  H   39
 0.40020000    1.83800000   18.60507000   4  H   40
-0.00712000   -0.28250000   18.69564000   3  C   41
 0.00116000   -0.26285000   20.10544000   5  N   42
 0.21745000    0.63350000   20.51516000   4  H   43
-0.22057000   -2.48930000   20.62852000   6  O   44
-0.11852000   -1.31878000   20.98318000   3  C   45
-0.79067000    1.10520000   22.26360000   4  H   46
-0.09830000   -0.94365000   22.43672000   3  C   47
-0.44771000    0.32071000   22.93260000   3  C   48
 0.50301000   -2.92806000   22.96561000   4  H   49
 0.26016000   -1.94355000   23.35031000   3  C   50
-0.41669000    0.58647000   24.29800000   3  C   51
-0.70402000    1.56816000   24.66218000   4  H   52
 0.30380000   -1.68495000   24.71478000   3  C   53
-0.03158000   -0.41336000   25.20177000   3  C   54
```

```
    0.59678000   -2.47416000   25.40064000   4  H   55
    0.00000000    0.00000000   26.93577000   2  S   56
    0.00000000   -2.88500000   29.25577000   1  Au  57
   -2.49850000   -1.44250000   29.25577000   1  Au  58
    2.49850000   -1.44250000   29.25577000   1  Au  59
    0.00000000    0.00000000   29.25577000   1  Au  60
   -2.49850000    1.44250000   29.25577000   1  Au  61
    2.49850000    1.44250000   29.25577000   1  Au  62
    0.00000000    2.88500000   29.25577000   1  Au  63
   -0.83280000   -1.44250000   31.61137000   1  Au  64
    1.66560000    0.00000000   31.61137000   1  Au  65
   -0.83280000    1.44250000   31.61137000   1  Au  66
    0.00000000   -2.88500000   33.96697000   1  Au  67
   -2.49850000   -1.44250000   33.96697000   1  Au  68
    2.49850000   -1.44250000   33.96697000   1  Au  69
    0.00000000    0.00000000   33.96697000   1  Au  70
   -2.49850000    1.44250000   33.96697000   1  Au  71
    2.49850000    1.44250000   33.96697000   1  Au  72
    0.00000000    2.88500000   33.96697000   1  Au  73
   -0.83280000   -1.44250000   36.32257000   1  Au  74
    1.66560000    0.00000000   36.32257000   1  Au  75
   -0.83280000    1.44250000   36.32257000   1  Au  76
    0.00000000   -2.88500000   38.67817000   1  Au  77
   -2.49850000   -1.44250000   38.67817000   1  Au  78
    2.49850000   -1.44250000   38.67817000   1  Au  79
    0.00000000    0.00000000   38.67817000   1  Au  80
   -2.49850000    1.44250000   38.67817000   1  Au  81
    2.49850000    1.44250000   38.67817000   1  Au  82
    0.00000000    2.88500000   38.67817000   1  Au  83
   -0.83280000   -1.44250000   41.03377000   1  Au  84
    1.66560000    0.00000000   41.03377000   1  Au  85
   -0.83280000    1.44250000   41.03377000   1  Au  86
    0.00000000   -2.88500000   43.38937000   1  Au  87
   -2.49850000   -1.44250000   43.38937000   1  Au  88
    2.49850000   -1.44250000   43.38937000   1  Au  89
    0.00000000    0.00000000   43.38937000   1  Au  90
   -2.49850000    1.44250000   43.38937000   1  Au  91
    2.49850000    1.44250000   43.38937000   1  Au  92
    0.00000000    2.88500000   43.38937000   1  Au  93
%endblock AtomicCoordinatesAndAtomicSpecies
```

References

(1) Zahid, F.; Paulsson, M.; Datta, S. In *Advanced Semiconductor and Organic Nano-Techniques III: Physics and Technology of Molecular and Biotechnology Systems*; Morkoç, H., Ed.; Academic Press: San Diego, 2003; Chapter 1 - Electrical Conduction through Molecules, pp 1 – 41.

(2) Economou, E. *Green's Functions in Quantum Physics*, 3rd ed.; Springer Series in Solid-State Sciences; Springer, 2006.

(3) Krstić, P. S.; Zhang, X.-G.; Butler, W. H. Generalized conductance formula for the multiband tight-binding model. *Phys. Rev. B* **2002**, *66*, 205319.

(4) Zhang, X.-G.; Krstić, P. S.; Butler, W. H. Generalized tight-binding approach for molecular electronics modeling. *Int. J. Quant. Chem.* **2003**, *95*, 394–403.

(5) Krstić, P. S.; Dean, D. J.; Zhang, X.-G.; Keffer, D.; Leng, Y. S.; Cummings, P. T.; Wells, J. C. Computational chemistry for molecular electronics. *Comput. Mater. Sci.* **2003**, *28*, 321 – 341.

(6) Quek, S. Y.; Venkataraman, L.; Choi, H. J.; Louie, S. G.; Hybertsen, M. S.; Neaton, J. B. Amine-gold linked single-molecule circuits: experiment and theory. *Nano Lett.* **2007**, *7*, 3477–82.

(7) Darancet, P.; Widawsky, J.; Choi, H.; Venkataraman, L.; Neaton, J. Quantitative Current-Voltage Characteristics in Molecular Junctions from First Principles. *NanoLett.* **2012**, *12*, 6250–6254.